The EMBO Journal vol.10 no.7 pp.1711 – 1722, 1991

A novel ATPase complex selectively accumulated upon heat shock is a major cellular component of thermophilic archaebacteria

Barry M.Phipps, Angelika Hoffmann[1], Karl O.Stetter[1] and Wolfgang Baumeister

Max-Planck Institute for Biochemistry, W-8033 Martinsried and [1]Department of Microbiology, University of Regensburg, W-8400 Regensburg, Germany

Communicated by W.Baumeister

We have discovered a large cylindrical protein complex which is an abundant component of the cytoplasm of extremely thermophilic archaebacteria. Structural analysis by image processing of electron micrographs suggests that the complex is composed of two stacked rings of eight subunits each; the rings enclose a central channel. The complex purified from the hyperthermophile *Pyrodictium occultum* is composed of equal quantities of two polypeptides of M_r 56 000 and 59 000. It exhibits an extremely thermostable ATPase activity with a temperature optimum of 100°C. The basal level of the ATPase complex in the cell is high, and it becomes highly enriched as a result of heat shock (shift from 102°C to 108°C) or balanced growth at temperatures near the physiological upper limit. Immunoblotting results indicate that a related protein is present in most thermophilic archaebacteria and in *Escherichia coli*. This protein complex may play an important role in the adaptation of thermophilic archaebacteria to life at high temperature.

Key words: ATPase/heat shock protein/protein structure/ring-shaped complex/thermophilic archaebacteria

Introduction

Archaebacteria constitute a third domain of life, consisting of organisms which live at extremes of temperature, pH and salt concentration. They are phylogenetically distinct from both the eubacteria and eukaryotes, although they possess some features of both kingdoms as well as many unique properties found in neither kingdom (Woese *et al.*, 1990). Members of the genus *Pyrodictium* are hyperthermophilic sulphur-reducing archaebacteria isolated from a submarine solphataric field near Vulcano, Italy (Stetter, 1982; Stetter *et al.*, 1983). They are among the most thermophilic organisms known to date, growing at up to 110°C and optimally at 105°C. An interesting question is how proteins in such organisms resist denaturation and operate stably at high temperature. This may be achieved by the acquisition of intrinsic structural stability (Jaenicke and Závodszky, 1990). Another possibility is that molecular chaperonins, of the kind originally proposed by Pelham (1986) and characterized in recent years (Hemmingsen *et al.*, 1988; Rothman, 1989), prevent or reverse the aggregation of denatured polypeptides and assist in their correct refolding.

In this report we describe an abundant, novel cytoplasmic protein complex in *Pyrodictium* and other thermophilic archaebacteria which appears as a ring with eight-fold symmetry in electron micrographs. Structural analysis by image processing reveals a cylindrical molecule composed of stacked discs of subunits. We report the purification of the complex from *Pyrodictium*, show that it is a remarkably thermostable and thermophilic ATPase and demonstrate that the level of the complex in the cell is elevated following heat shock. Related molecules span a large phylogenetic distance, suggesting that the complex performs a conserved function.

Results

Electron microscopy of the Pyrodictium eight-fold symmetric complex

In the course of isolating *Pyrodictium brockii* cell envelopes by freeze–thaw lysis of whole cells and examining the preparation by electron microscopy, bursts consisting of a large number of particles, ring-shaped and striated, were found adjacent to large envelope fragments. A micrograph of such a burst of particles is shown in Figure 1A, and galleries of images of the single particles in Figure 1B and C. The envelope fragments appeared to derive from the rupture of individual cells and most likely represent cells that remained unbroken after the freeze–thaw procedure and subsequently lysed on the electron microscope grid, releasing cytoplasmic contents next to the ruptured cell. The large amount of the material apparently released by a single lysis event indicates that it represents an abundant cellular component. The ring-shaped and the striated species copurify (described below) and are therefore likely to represent different orientations of the same macromolecular complex. We have designated these end-on views (ring-shaped) and side-on views (striated), respectively. End-on views (Figure 1B) comprise a central stain-filled region enclosed by a ring in which eight segments can sometimes be discerned. In the side-on views (Figure 1C) one can see four striations, two strong ones in the centre and two weak ones peripherally. When orientated as shown, the upper and lower halves appear to be equivalent, as do the left and right halves. Complexes in the side-on orientation frequently associate into short chains, in a side-to-side fashion (Figure 1A, single arrows). These chains exhibit some tendency to stack such that the complexes are aligned both side-to-side and top-to-bottom (Figure 1A, double arrow).

Image analysis

The impression that end-on views of the complex possess eight-fold symmetry was tested by extracting several images of single particles and subjecting them to rotational correlation analysis. Plots of correlation coefficients versus rotation angle for three particles are displayed in Figure 2. In each case, eight correlation peaks spaced ~45° apart are observed, confirming that the complex is eight-fold symmetric, at least at this level of resolution.

In order to gain further information about the structure

of the complex, end-on and side-on views of single particles were separately selected from several micrographs and subjected to single particle averaging using correlation methods. An average of 264 end-on views is displayed in Figure 3A. A ring of eight equally spaced globular masses surrounds a stain-filled centre. The diameter of the ring is 16 nm and of the central hole is 5 nm.

Figure 3B shows the result of averaging 284 individual

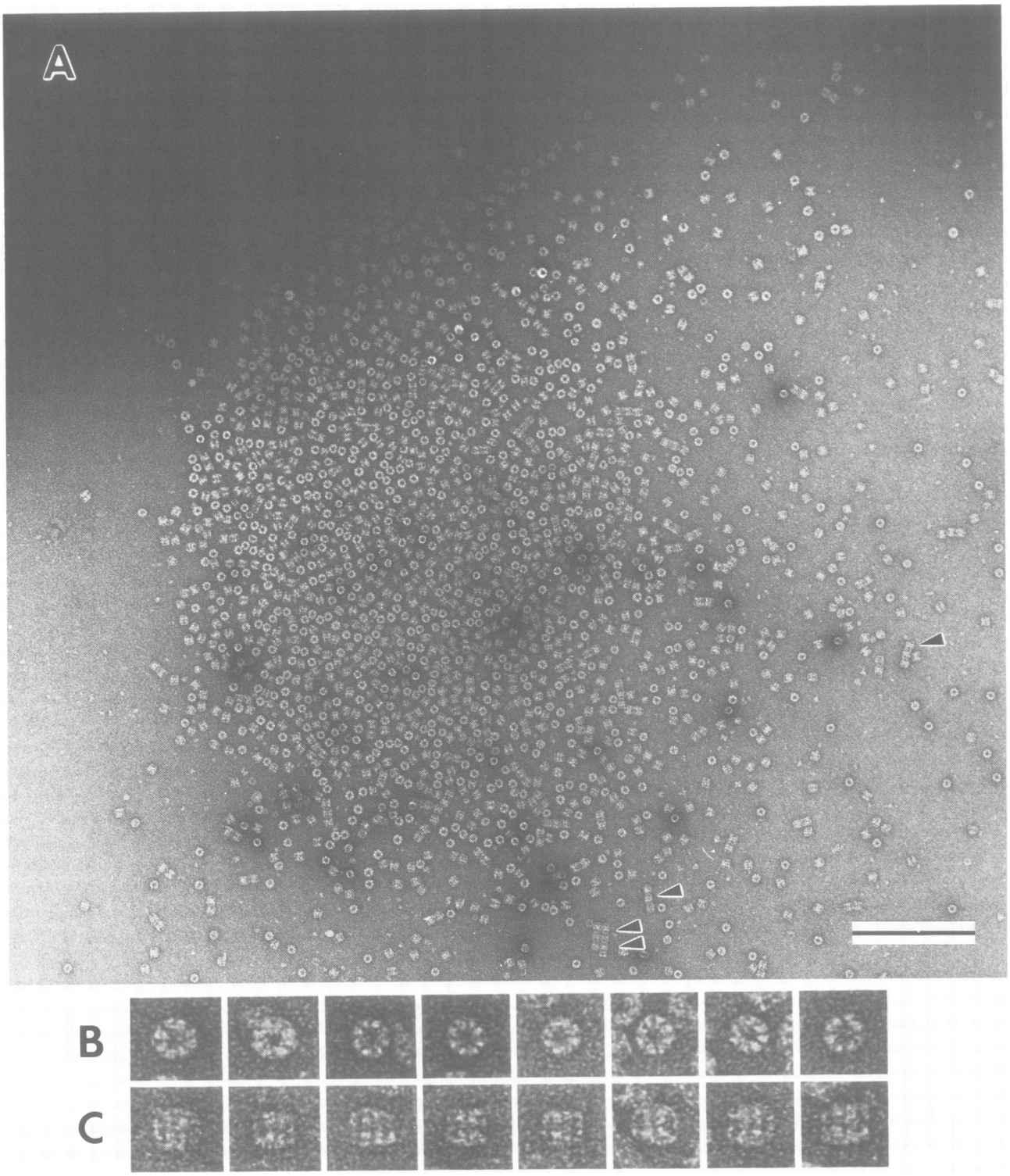

Fig. 1. Electron microscopy of *P.brockii* eight-fold symmetric particles. (**A**) Micrograph of a burst of particles released from what was probably a whole cell (dark staining area at upper left) which lysed on the carbon foil. The preparation consisted of cell envelopes and unbroken cells prepared by freeze–thaw lysis of whole cells, and was stained with uranyl acetate. The particles comprise almost exclusively ring-shaped end-on views and rectangular, striated side-on views. Single arrows point to chains of side-on views orientated such that the striations of the constituent particles are parallel. Double arrow indicates a small 2-D array in which side-on views are aligned side-to-side and top-to-bottom. Bar = 200 nm. (**B,C**) Galleries of single particle images selected interactively from a computer graphics display of the micrograph in (A). (B) End-on views. (C) Side-on views.

side-on views. The maximum width (X) and height (Y) of the average are 16.5 nm and 15.5 nm, respectively. An axis of two-fold rotational symmetry passes through the centre of the complex in this projection. Each of the four vertical striations is resolved into distinct upper and lower centres of mass. The equivalent upper and lower halves of the complex appear to be well-defined independent structural units; a band of low density (i.e. stain accumulation) occurs where the inner faces of these structures meet. Each half consists of two strong globular masses towards the centre of the complex and two weak masses located at the periphery. It should be noted that, at this low level of resolution, it is impossible to say whether or not structural features which appear to be equivalent are truly symmetry related.

Electron microscopy of a similar complex from other thermophilic archaebacteria

We have observed a similar complex in other thermophilic archaebacteria as well. *Thermoplasma acidophilum* is a thermoacidophile growing optimally at 59°C (Darland *et al.*, 1970). Figure 4A is a micrograph of a fraction encountered during the purification of another macromolecular complex, the proteasome or multicatalytic proteinase, from *T.acidophilum* (Dahlmann *et al.*, 1989). Unlike the *P.brockii* sample, the *Thermoplasma* preparation contained a mixture of several different particles. However, the predominant species was ring-shaped. We 'purified' this species at the level of image processing by interactively selecting the images of 128 such particles and subjecting them to correlation-based averaging. The result, shown in Figure 4B, reveals a ring with eight distinct uniformly-spaced centres of mass. The diameter of the complex is 15 nm; the central cavity measures 6 nm across, slight larger than for *Pyrodictium* and *Archaeoglobus* (see below). Corresponding side-on views were rarely seen; one is marked with a single arrow in Figure 4A. The major striated species observed in these preparations, indicated by the double arrow in the figure, are identified as proteasomes by their characteristic reel-shaped structure and dimensions of ~11 nm in width and 15 nm in length (Dahlmann *et al.*, 1989). In addition, contaminating macromolecular species of less distinctive shape are present in the fraction.

Archaeoglobus fulgidus is an extremely thermophilic, weakly methanogenic, sulphate-reducing archaebacterium with a growth temperature optimum of 83°C (Stetter *et al.*, 1987; Stetter, 1988). Cytoplasmic contents released by freezing and thawing whole cells were negatively stained and examined. The micrograph in Figure 4C contains primarily rings with eight-fold symmetry. An average of 137 such particles is displayed in Figure 4D. The diameter of the complex is 16 nm and of the cavity is 5 nm. Side-on views are also rare in this preparation; one is indicated by the arrow in Figure 4C.

Purification of the Pyrodictium complex

Pyrodictium occultum possesses an apparently eight-fold symmetric complex which is indistinguishable from that of *P.brockii*. We purified the complex to homogeneity (Figure 4E). A detailed description of the purification scheme can be found in Materials and methods. In the course

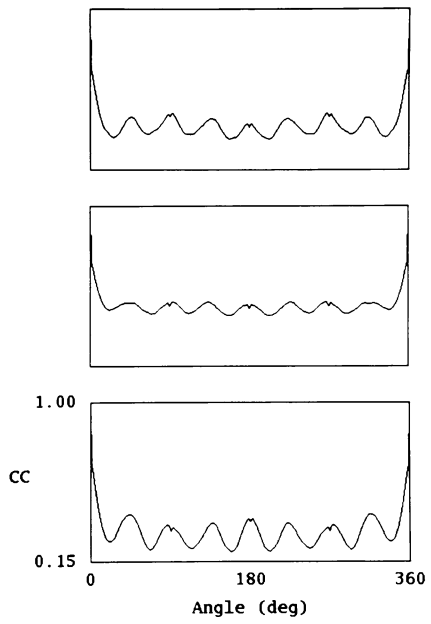

Fig. 2. Rotational correlation of end-on views of the *P.brockii* complex. The top, middle and bottom correlation plots correspond to the first, second and third images in Figure 1B. Correlation coefficients (CC) on the vertical axis (0−1) are plotted against the angle by which the image was rotated. The mean angular distance between adjacent peaks is 45.0 ± 3.2°.

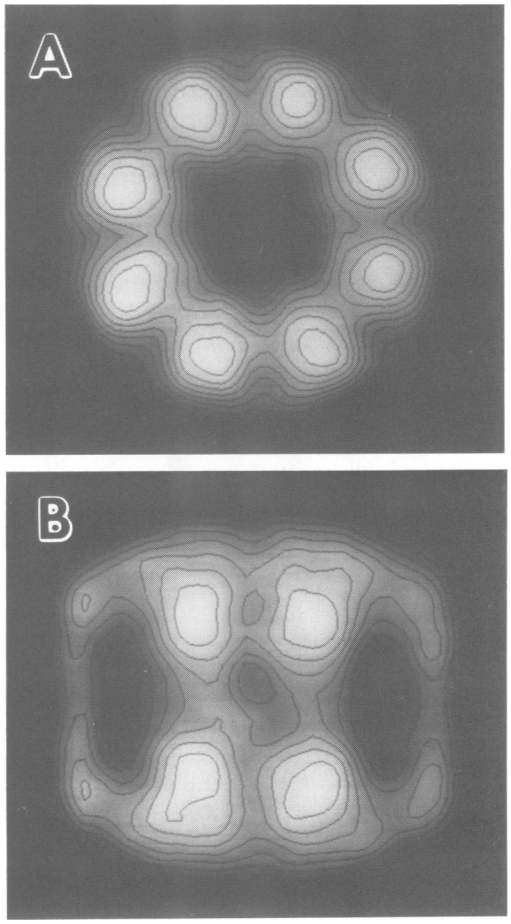

Fig. 3. Correlation averages of the *P.brockii* complex. (**A**) Average of 264 end-on views. Diameter of ring = 16 nm; diameter of central hole or depression = 5 nm. (**B**) Average of 284 side-on views. Maximum height = 15.5 nm; maximum width = 16.5 nm. No symmetrization was applied in either case.

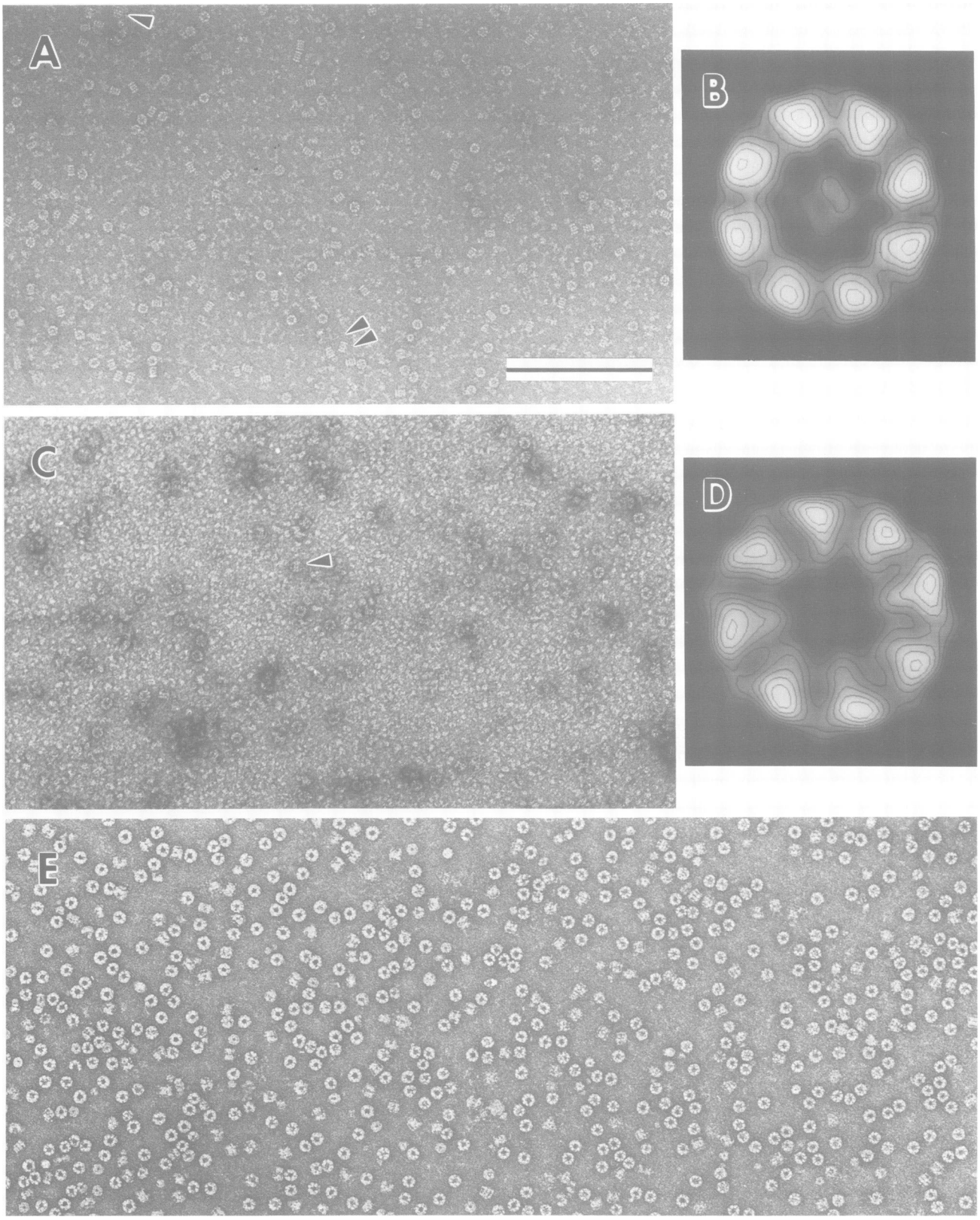

Fig. 4. Electron microscopy of eight-fold symmetric complexes from *Thermoplasma* and *Archaeoglobus* and purified complex from *P.occultum*. **(A)** Complex-containing fraction obtained during the purification of proteasomes from *Thermoplasma acidophilum*, stained with ammonium molybdate. The ring-shaped particles correspond to end-on views of the complex. The single arrow points to a side-on view. The predominant rectangular, striated particles are proteasomes; some are indicated by the double arrow. Bar = 200 nm. **(B)** Correlation average of 128 end-on views of the *Thermoplasma* complex. Diameter of ring = 15 nm; diameter of hole = 6 nm. No symmetrization was applied. Weak positive density of irregular shape occurring in the central stain-filled hole most likely results from incomplete filling of the hole or depression with stain. **(C)** Crude soluble protein extract of *Archaeoglobus fulgidus* cells, obtained by freeze–thaw lysis and stained with uranyl acetate. The rings are end-on views of the complex; the arrow indicates a side-on view. **(D)** Correlation average of 137 end-on views of the *Archaeoglobus* complex. Diameter of ring = 16 nm; diameter of hole = 5 nm. No symmetrization was applied. **(E)** Purified complex isolated from *P.occultum*.

of isolation it was discovered that the complex possesses ATPase activity. Thus, while the definitive assay for the presence of the complex during purification was its appearance in the electron microscope, ATPase activity was also followed at all stages. The results of the major purification steps are illustrated in Figure 5. Initially, macromolecules of high mol. wt were concentrated between purification steps by ultracentrifugation. However, it was found that, when pelleted, the complex formed aggregates that were very difficult to resolubilize. This problem was avoided by using ultrafiltration to concentrate the samples. Membrane-free French press lysate was fractionated on a DEAE−Sephacel anion exchange column (Figure 5A). The complex eluted between 200 and 300 mM KCl and was resolved by ultracentrifugation on successive sucrose/glycerol and glycerol gradients (Figure 5B and C). The complex banded in the 18−21% sucrose/7−8% glycerol range of the first gradient and in the 28−32% glycerol range of the second. At each stage, the complex comigrated with the largest peak of protein mass and ATPase activity, indicating that it is an abundant cytoplasmic protein. Finally, the protein was chromatographed on an FPLC Mono-S cation exchange column which retained minor contaminants but allowed the complex to pass unretarded. The result was a homogeneous preparation of the complex as judged by electron microscopy (Figure 4E) and SDS−PAGE (Figure 6, lane f). A yield of ~0.75 mg of purified protein with a specific ATPase activity of 0.41 U/mg was obtained from 20 g (wet wt) of cells. This represents 0.7% of the total soluble protein.

The purified complex yields two bands of equal staining intensity and M_r 56 000 and 59 000 in SDS−PAGE (Figure 6, lane f). The gel shows that the major purification was achieved by the two gradient centrifugation steps (Figure 6, lanes d and e). The DEAE column provided a two- to three-fold increase in purity (Figure 6, lane c). Furthermore it served to concentrate the protein sample and to remove the large amount of DNA and RNA present in the cytoplasm (nucleic acids bind very tightly to the column) without resorting to the use of DNase and RNase. The latter was important since nucleic acid is sometimes found as a component of large macromolecular complexes, e.g. proteasomes (Arrigo *et al.*, 1987) and signal recognition particles (Siegel and Walter, 1988). Densitometry of the ATPase bands in whole cell lysates (Figure 6, lane b) indicates that the complex constitutes approximately 8% of the total

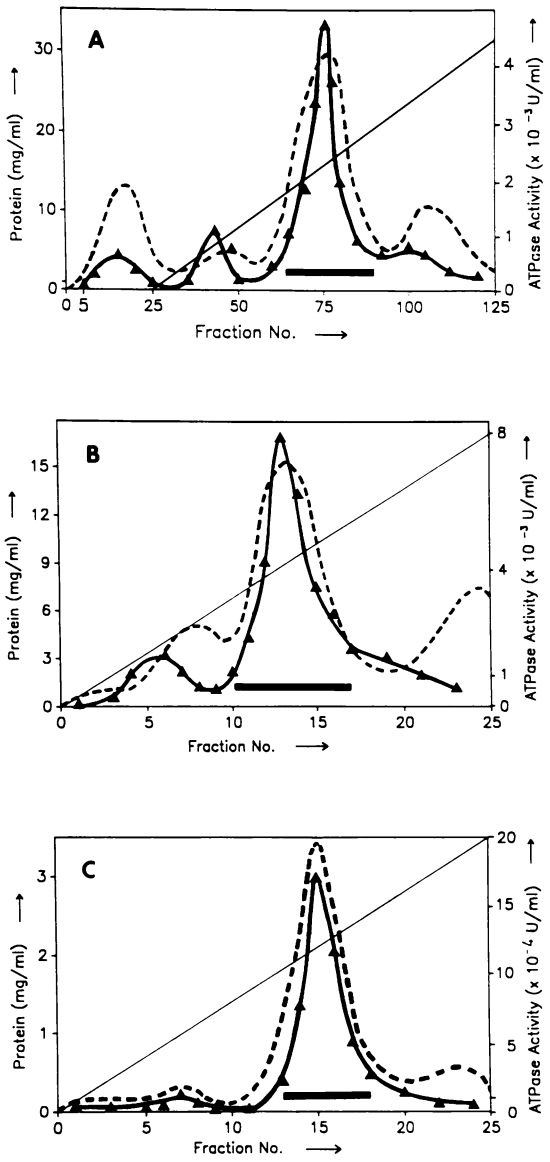

Fig. 5. Purification of the ATPase complex from *P.occultum*. (**A**) DEAE-Sephacel chromatography of membrane-free cell lysate. Bed volume = 100 ml. Elution was achieved with a gradient of 50−500 mM KCl, represented by the thin line. The complex eluted between 200 and 300 mM KCl. Volume/fraction = 8 ml. (**B**) Sucrose−glycerol density gradient centrifugation of pooled fractions from the DEAE column. The linear gradient of 10−30% sucrose and 5−10% glycerol is indicated by the thin line. The complex eluted in the 18−21% sucrose/7−8% glycerol range. Volume/fraction = 0.5 ml. (**C**) Glycerol density gradient centrifugation of pooled fractions from the sucrose−glycerol gradient. The linear gradient of 18−37% glycerol is represented by the thin line. The complex eluted in the 28−32% glycerol range. Volume/fraction = 0.5 ml. Fractions were assayed for ATPase activity at 100°C (▲−▲) and their protein content estimated by absorbance at 280 nm (---). Fractions pooled at each stage are indicated by a solid bar.

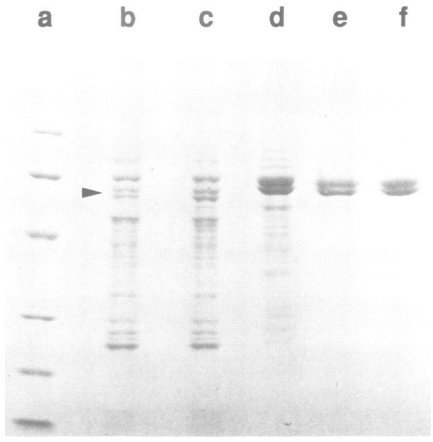

Fig. 6. Pooled *P.occultum* ATPase complex at different stages of purification. An aliquot of sample containing 20 μg of protein (lanes b−f) was loaded in each well of an SDS gel. Lane a, mol. wt standards: phosphorylase b (97 400); serum albumin (66 200); ovalbumin (45 000); carbonic anhydrase (31 000); trypsin inhibitor (21 500); lysozyme (14 400). Lane b, membrane-free cell lysate. Lane c, pooled complex-containing fractions from DEAE−Sephacel column. Lane d, pooled fractions from sucrose−glycerol gradient. Lane e, pooled fractions from glycerol gradient. Lane f, pooled fractions from Mono-S column. The arrow indicates the position of the two ATPase bands in lanes b and c, where they migrated slightly farther than in lanes d−f.

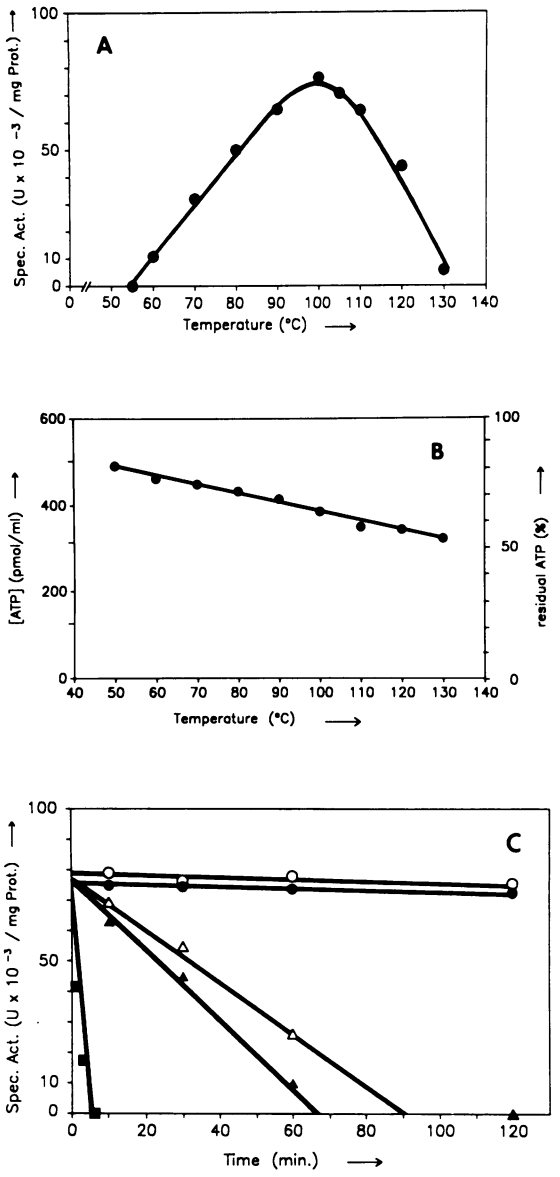

Fig. 7. Temperature dependence and thermal stability of purified ATPase complex. (**A**) ATPase activity as a function of temperature. Samples were incubated for 1 min at the appropriate temperature. (**B**) Spontaneous hydrolysis of ATP at high temperature. The amount of ATP remaining after a 1 min incubation in ATPase assay buffer (no enzyme) is plotted against temperature. The starting concentration of ATP was 600 pmol/ml. (**C**) Thermostability of the ATPase. Samples were pre-incubated at different temperatures for various periods of time in ATPase assay buffer containing no ATP. ATPase activity was then assayed by adding ATP and incubating at 90°C for 1 min. Samples were not taken at 0 time; curves were extrapolated to the ordinate. 90°C, ○−○; 110°C, ●−●; 100°C, △−△; 120°C, ▲−▲; 130°C, ■−■.

cytoplasmic protein. That this is considerably higher than the yield of the purification is not surprising since the tendency of the complex to form aggregates would be expected to result in significant losses.

ATPase activity

The purified complex has a strong ATPase activity which is strictly dependent on high temperature. Figure 7A depicts the activity as a function of temperature. Optimal activity occurs at 100°C. The enzyme is still at least 50% active over the range 80−120°C. An unusual feature of the

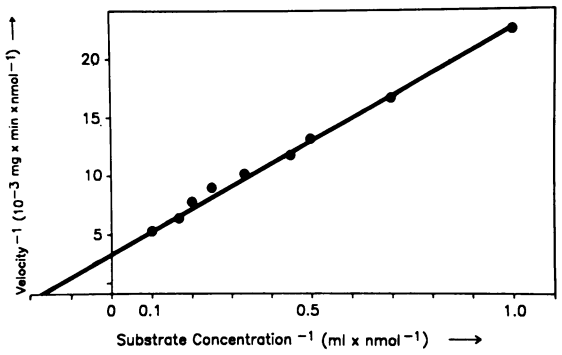

Fig. 8. Lineweaver−Burk analysis of ATPase activity of the purified complex. Samples were incubated for 5 min at 90°C. V_{max} = 0.29 U/(mg protein) and K_m = 5.6 μM.

temperature dependence is that it is approximately linear in the range 55−90°C. Normally, one would expect to see an exponential Arrhenius dependence until the enzyme begins to suffer thermal denaturation effects near and above the temperature optimum (Roberts, 1977).

An important point to keep in mind when conducting ATPase assays at high temperature is that the rate of spontaneous hydrolysis of ATP is enhanced with increasing temperature. We therefore determined the amount of ATP hydrolysed as a function of temperature under normal assay conditions but in the absence of the enzyme complex. The results (Figure 7B) show that significant ATP breakdown does occur and that it increases as a function of the assay temperature. In all activity calculations presented here, the amount of spontaneous hydrolysis has been corrected for.

In order to understand the mechanistic reasons behind the temperature dependence of the enzyme, we incubated the complex at different temperatures for various periods of time and then determined its residual ATPase activity. The results are displayed in Figure 7C. The enzyme is remarkably thermostable. No diminution of ATPase activity is observed after prolonged treatment at 90°C or 100°C. At 110°C and 120°C, significant activity remains even after incubating for 1 h, but further incubation leads to the irreversible loss of ATPase function. When the temperature is increased to 130°C, the enzyme is completely inactivated in < 10 min. Thus it appears that the gradual reduction in ATPase activity at temperatures > 100°C is due to thermal inactivation of the enzyme.

A Lineweaver−Burk plot for the activity of the *P.occultum* ATPase at 90°C and pH 7.5 is given in Figure 8. It yields a value for V_{max} of 0.29 U/(mg protein) and for K_m of 5.6 μM, indicating an unusually high affinity for substrate. The turnover number is 5 s^{-1}. The complex was shown to be an ATPase and not a pyrophosphorylase by subjecting reaction products to chromatography on an HPLC μ-Bondabak NH2 column (anion exchanger, Waters); the only nucleotide generated by the reaction is ADP (data not shown).

The complex is preferentially accumulated following heat shock

Living organisms including archaebacteria respond to an upshift in temperature by elevating the synthesis of a defined set of cellular proteins, known as heat shock proteins, and accumulating them to higher steady state levels (Lindquist, 1986; Neidhardt and VanBogelen, 1987). The heat shock response is an aid to the growth and survival of cells at

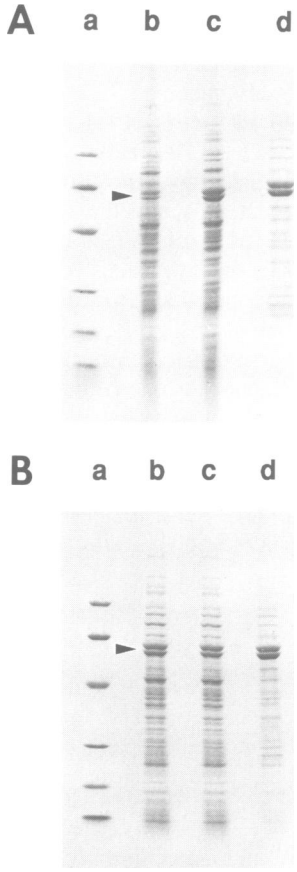

Fig. 9. Selective accumulation of *P.occultum* ATPase complex in response to heat shock. (**A**) Steady state growth: SDS−PAGE of membrane-free lysates of *P.occultum* cells grown to exponential phase at different temperatures. Lane b, 90°C. Lane c, 100°C. Lane d, 108°C. (**B**) Heat shock: SDS−PAGE of membrane-free lysates of *P.occultum* cells. Lane b, cells grown to exponential phase at 102°C. Lane c, cells kept at 102°C and incubated for 4 h. Lane d, cells shifted to 108°C and incubated for 4 h. In both experiments, 20 μg of total protein was loaded in each sample well. Lane a in both panels contains molecular weight standards: phosphorylase b (97 400); serum albumin (66 200); ovalbumin (45 000); carbonic anhydrase (31 000); trypsin inhibitor (21 500); lysozyme (14 400). Arrows point to the pair of ATPase bands.

temperatures higher than their normal physiological range. An interesting question is whether or not archaebacteria that normally grow at very high temperatures exhibit such a response. We first examined the steady state levels of soluble proteins as a function of growth temperature by growing *P.occultum* cells to late exponential phase at 90°C, 100°C and 108°C. Figure 9A shows an SDS gel of the total soluble protein from these cells. It is clear that, under steady state conditions, the relative level of the ATPase increases with increasing growth temperature. Furthermore, the levels of most other proteins decrease, especially when the temperature is increased from 100°C to 108°C. At 108°C the ATPase constitutes 73% of the total soluble protein compared with 11% at 100°C and 6% at 90°C, as judged by densitometry. Thus, at very high temperatures, the cytoplasmic protein consists predominantly of this single species, suggesting that it may play an important role in the ability of the cells to withstand extreme heat.

In order to examine the effect of heat shock on the protein composition cells were grown to exponential phase at 102°C and portions of the culture further incubated at 102°C or shifted to 108°C. The results are displayed in Figure 9B. After 4 h growth at the same temperature, no change in the protein profile is seen (lane c). However, 4 h after shifting to the higher temperature the ATPase accounts for a significantly larger fraction of the total soluble protein (lane d), ~35% as compared to 13% for the unshifted cells. We conclude that the ATPase complex is preferentially accumulated in response to heat shock in *P.occultum*, and that this leads to the establishment of a higher relative steady state level of the protein. These experiments do not allow us to decide whether this is due to an elevated rate of synthesis of the ATPase, a reduced rate of synthesis of other cytoplasmic proteins or enhanced degradation of the latter.

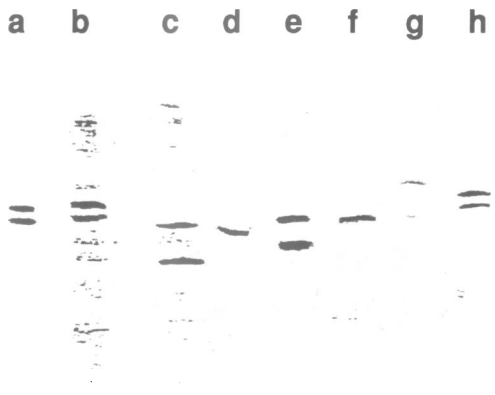

Fig. 10. Immunological cross-reaction of soluble proteins of archaebacteria and eubacteria with antiserum against purified ATPase complex. An aliquot of membrane-free cell lysate containing 5 μg of protein was loaded in each well of an SDS gel. Proteins were transferred to nitrocellulose and probed with antiserum against purified *P.occultum* ATPase at a dilution of 1:10 000. Lane a, purified *P.occultum* ATPase complex. Lane b, *Pyrodictium occultum*. Lane c, *Sulfolobus acidocaldarius*. Lane d, *Archaeoglobus fulgidus*. Lane e, *Thermoplasma acidophilum*. Lane f, *Methanothermus fervidus*. Lane g, *Methanoplanus limicola*. Lane h, *Escherichia coli*.

Presence of the complex in thermophilic archaebacteria

Membrane-free French press lysates of several archaebacteria, the eubacteria *E.coli* and *Thermotoga maritima* and the yeast *Saccharomyces cerevisiae* were electrophoresed in SDS gels and probed by immunoblotting with antiserum raised against the *P.occultum* ATPase complex. The results are displayed in Figure 10 and summarized in Table I. The reaction of the pair of bands in *P.occultum* (lane b) confirms that the protein exists in the cell as two polypeptides of similar mol. wt, i.e. this is not the result of proteolysis during purification. Varying degrees of cross-reaction were observed with one or more protein bands in the 60 kd region. A positive cross-reaction was found with most of the extremely thermophilic archaebacteria tested, which were chosen to span the full phylogenetic breadth of this group of organisms. A strong cross-reaction was found with *Archaeoglobus fulgidus* (lane d) and *Thermoplasma acidophilum* (lane e), in good agreement with the electron microscopic observations of similar complexes in these species. Little or no signal was observed with the extremely halophilic or methanogenic archaebacteria, with the exception of *Methanothermus fervidus* (lane f), an extremely

Table I. Immunological cross-reaction of cell lysates of various organisms with antiserum against *P.occultum* ATPase complex

Organism	Cross-reaction
Extremely thermophilic archaebacteria	
Pyrodictium occultum PL-19	+++
Pyrodictium abyssi AV2	+++
Pyrodictium sp. 1A	+++
Acidianus brierleyi	++
Archaeoglobus fulgidus VC-16	++
Archaeoglobus profundus AV18	++
Desulfurococcus amylolyticus Z-533	(+)
Pyrobaculum islandicum GEO3	+
Pyrococcus furiosus VC1	(+)
Staphylothermus marinus F1	++
Sulfolobus acidocaldarius 98-3	+++
Thermococcus litoralis NS-C	(+)
Thermofilum librum V24N	−
Thermoplasma acidophilum 122-1B2	+++
Halophilic and methanogenic archaebacteria	
Halobacterium halobium	−
Halococcus morrhuae L.D.3.1	−
Methanococcus thermolithotrophicus SN1	−
Methanococcus igneus Kol5	−
Methanoplanus limicola M3	(+)
Methanopyrus sp. AV19	−
Methanothermus fervidus V24S	++
Eubacteria	
Escherichia coli	+
Thermotoga maritima MSB8	−
Yeast	
Saccharomyces cerevisiae	−

Cross-reactions were determined by immunoblotting as described in the legend to Figure 10. The reactions with *Desulfurococcus amylolyticus*, *Pyrococcus furiosus* and *Thermococcus litoralis* were only observed when a lower antiserum dilution (1:3000) was used.

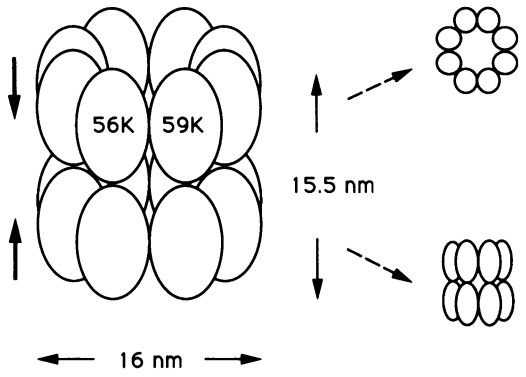

Fig. 11. A model of the *Pyrodictium* ATPase complex. The model consists of two stacked rings of eight ellipsoidal subunits each, the rings being oppositely orientated such that equivalent faces are in contact. It is traversed by a central channel of diameter 5 nm. The complex is composed of an equimolar combination of 56 kd and 59 kd polypeptides which we suggest to alternate in each ring, each polypeptide corresponding to a single subunit. The right side of the figure shows how ring-shaped (top) and rectangular striated (bottom) views are generated by viewing the complex in end-on and side-on orientations, respectively.

thermophilic methanogen (Stetter *et al.*, 1981). Neither the thermophilic eubacterium *Thermotoga maritima* nor yeast cells reacted with the antiserum.

Interestingly, a significant signal was detected with a pair of bands of M_r 59 000 and 62 000 in *E.coli* (lane h). The abundant *E.coli* heat shock protein groEL has a subunit M_r of 57 259 (Hemmingsen *et al.*, 1988), although values determined from its migration on SDS gels vary from 57 000 to 65 000 (Neidhardt *et al.*, 1981; Hendrix, 1979). In addition, it possesses ATPase activity and is a cylindrical oligomer of comparable size to the *Pyrodictium* ATPase, but is distinctly different in symmetry and mass distribution (Hendrix, 1979; Hohn *et al.*, 1979). Thus it is possible that one of the two cross-reacting bands corresponds to groEL. Immunoblotting of purified *Pyrodictium* ATPase with polyclonal antiserum against groEL (generously provided by R.Jaenicke, University of Regensburg, Germany) resulted in a very weak reaction of one of the two ATPase bands (data not shown). To achieve a level of cross-reactivity comparable with that of the homologous groEL protein, ~20 times as much protein was required. Whether this reaction results from the presence of structurally similar epitopes in the two proteins is not clear.

Discussion

We have discovered a large protein complex with apparent eight-fold symmetry to be a major component of at least three thermophilic archaebacteria, and immunoblotting results suggest that related molecules span a phylogenetic spectrum which includes the archaebacteria and eubacteria. The purified complex isolated from *Pyrodictium* is an ATPase with maximal activity at 100°C. Since the complex is found in membrane-free whole cell lysates, it is probably a component of the cytoplasm. The complex is an abundant constitutive component of the cell and, in addition, its level relative to other cytoplasmic proteins is dramatically elevated in response to heat shock or balanced growth at extreme temperature.

An advantage of single particle image selection and averaging techniques is that they permit one to obtain structural information about a macromolecular species before biochemical purification methods have been applied. Thus one can 'purify' the protein by image processing, as long as it is sufficiently unique in appearance to be distinguished from contaminating species. This enabled us to determine the projection structure of the complex from crude cytoplasmic extracts of *Thermoplasma* and *Archaeoglobus*, as well as from *Pyrodictium* preparations containing envelopes and whole cells.

A simple working model of the complex based on the *P.brockii* averages is presented in Figure 11. We assume that the upper and lower halves of the side-on view correspond to two rings of eight globular protein subunits each. The rings are stacked on top of each other to form a cylinder of height 15.5 nm and width 16 nm, which is traversed by a central channel. We further assume that the rings are asymmetric in the Y direction and that equivalent faces of the two rings are in contact, to account for the apparent asymmetry seen in side-on views. However, this asymmetry could result from differential staining of the outside and inside of the complex, and not from any inherent asymmetry in the protein ring. End-on views result from looking down onto the top of the cylinder which is standing on one end. Side-on views are generated when the cylinder is lying on its side; four protein subunits from each of the two rings

are visible, but the laterally located subunits are less prominent.

We emphasize that this is only a working model. It is quite possible, for instance, that the width (X axis) of the side-on view corresponds to the long axis of the cylinder and the height to its diameter. In this case the complex might be made up of four rings, two large rings centrally and two small rings peripherally, or of two double-rings in which each protein subunit has distinct folding domains which contribute to the non-equivalent parts of the double-ring.

From the dimensions of the averages of the *P.brockii* complex and assuming that the working model correctly represents the structure, one can calculate a rough M_r of 1.1×10^6 for the complex (protein density = 1.3 g/cm^3). An assembly of 16 subunits of mean M_r 57 500 would have an M_r of 0.9×10^6. Thus it is likely that each ellipsoidal subunit in the model corresponds to a single 56 kd or 59 kd polypeptide. This, and the fact that they are so close in molecular weight, suggest some similarity in the structure of the two polypeptides. However, it should be noted that only gross structural differences can be discerned at the level of resolution attained in this study. We suggest that the 56 kd and 59 kd monomers might alternate in the eight-subunit ring, as shown in Figure 11. In this case, each ring would be a tetramer of heterodimers and the true symmetry of the complex would be four-fold rather than eight-fold. By applying single particle 3-D reconstruction by means of quasi-conical tilting (currently in progress) and preparation techniques ensuring better structural preservation, such as embedding in aurothioglucose, it may be possible to detect structural differences between the subunits. The tendency of side-on orientated complexes to stack in an aligned fashion (Figure 1A) offers the hope that the complex can be induced to form 2-D crystals under the appropriate conditions, which would allow 3-D structural analysis by the established methods of electron crystallography.

A structural motif common to several large oligomeric protein complexes is a stack of two or more rings or discs of structurally similar or identical protein subunits. Eukaryotic and *Thermoplasma acidophilum* proteasomes are believed to be composed of two large rings with two smaller rings sandwiched between them; the rings are composed of structurally related subunits (Kopp *et al.*, 1986; Baumeister *et al.*, 1988; Dahlmann *et al.*, 1989; Lilley *et al.*, 1990). The heat shock-inducible chaperonins, *E.coli* groEL and mitochondrial hsp60 and the chloroplast homologue known as Rubisco subunit binding protein, comprise double rings of seven monomers each (Hendrix, 1979; Hohn *et al.*, 1979; Pushkin *et al.*, 1982; McMullin and Hallberg, 1988; Hutchinson *et al.*, 1989). Alpha-2 macroglobulin appears to be constructed from two pseudotetrameric (actually dimeric) ring-like structures, each of which is a functional half-molecule (Feldman *et al.*, 1985). The data presented here suggest a similar organizational principle for the archaebacterial ATPase complex. The reasons for such an arrangement are not known. However, we have evidence that some of the complexes mentioned above reversibly dissociate into half molecules (W.Baumeister, A.Grziwa and G.Pfeifer, unpublished results). It may be that the functional activity of large complexes is regulated by an equilibrium between associated and dissociated rings, possibly mediated by ATP binding and/or hydrolysis. One face of a ring may bear a site for substrate binding or enzymatic activity, which becomes buried upon assembly of the rings into the holoenzyme. Such a regulatory mechanism might be important for prokaryotic cells, which cannot control enzyme activity by means of organellar compartmentalization.

The thermostability and temperature optimum of the *Pyrodictium* ATPase are among the highest known for an enzyme. This is perhaps not surprising since *Pyrodictium* shares with members of the genera *Methanopyrus* (Huber *et al.*, 1989) and *Hyperthermus* (Zillig *et al.*, 1990) the distinction of growing at a higher temperature than any other organism (110°C). The activity of the ATPase is maximal at 100°C, which is only slightly less than the growth optimum of the organism (Stetter *et al.*, 1983). The ATPase adds to a growing number of extremely thermophilic enzymes which have been isolated from thermophilic archaebacteria (Prangishvilli *et al.*, 1982; Pihl *et al.*, 1989; Costantino *et al.*, 1990; Eggen *et al.*, 1990). The high specific activity of the ATPase and the exceptionally strong affinity it has for ATP (K_m = 5.6 μM) may be adaptations allowing the enzyme to 'compete' successfully with hydrolysis for ATP.

As far as we know, this is the first documentation of a heat shock response in a hyperthermophile. Jerez (1988) and Trent *et al.* (1990) demonstrated the preferential synthesis of a subset of proteins under heat shock conditions in *Sulfolobus*, an archaebacterium with a growth temperature optimum of approximately 80°C. Both studies found that, in SDS gels, most cytoplasmic proteins were radically diminished while, depending on the species of *Sulfolobus* examined, one major band (55 kd) or a pair of major bands close in molecular weight (64 kd and 66 kd) were preferentially expressed. This is reminiscent of our results obtained with *Pyrodictium*. Unfortunately, these heat shock proteins were not isolated or characterized further, precluding a comparison with the *Pyrodictium* enzyme. Interestingly, in an immunoblot with antiserum against the *P.occultum* ATPase (Figure 10) a reaction was observed with a pair of *Sulfolobus acidocaldarius* polypeptide bands in the 50–60 kd range. Thus it is possible that the major heat shock proteins of *Sulfolobus* are related to the *Pyrodictium* ATPase.

The electron microscopic and immunoblotting results suggest that the ATPase complex is a feature of thermophilic archaebacteria. Nevertheless, these thermophiles span a large phylogenetic distance which includes both major lineages of the archaebacteria (Klenk *et al.*, 1986; Woese *et al.*, 1990). Of course, the negative immunoblotting results with the halophiles and methanogens do not necessarily imply that a similar complex is absent from these organisms. The positive reaction with *E.coli* raises the possibility that the complex is a member of a widely distributed conserved superfamily of proteins.

We do not yet know what the function of the ATPase complex is. However, the abundance of the protein, its response to heat shock and growth at high temperature, and its broad distribution among thermophilic archaebacteria suggest that it might play an important role in the adaptation of these organisms to life at high temperature. Interestingly, the ATPase exhibits a number of similarities with the oligomeric groEL protein of *E.coli* and its homologues from mitochondria (hsp60) and chloroplasts (Rubisco subunit binding protein). These consist of 60 000 M_r subunits

which assemble into complexes that comprise two stacked rings, each containing seven subunits. They yield end-on and side-on views in the electron microscope which are superficially similar to those observed in this study; however end-on views exhibit seven-fold rather than eight-fold symmetry and the detailed mass distribution in both views is different (Hendrix, 1979; Hohn *et al.*, 1979; Pushkin *et al.*, 1982; McMullin and Hallberg, 1988). While groEL and hsp60 are composed of a single type of subunit, the Rubisco subunit binding protein is made up of equal quantities of dissimilar monomers which are very close in molecular weight (Musgrove *et al.*, 1987; Martel *et al.*, 1990), analogous to the *P.occultum* ATPase. The *Pyrodictium* complex and groEL are highly expressed and are accumulated to even higher levels following heat shock or during balanced growth at high temperatures (Lemaux *et al.*, 1978; Herendeen *et al.*, 1979; Neidhardt *et al.*, 1981). Mitochondrial hsp60 is also induced by heat shock (McMullin and Hallberg, 1987; Reading *et al.*, 1989). GroEL and hsp60 are ATPases and the turnover number for groEL of 1.4 s^{-1} (Viitanen *et al.*, 1990) is comparable to that of the *Pyrodictium* enzyme. Two ~60 kd bands in *E.coli* lysates react with antiserum against the *P.occultum* complex; it remains to be shown whether or not one of these bands corresponds to groEL. One of the ATPase subunits reacted weakly with anti-groEL antibody. The above observations suggest a possible relationship between the *Pyrodictium* ATPase and the groEL family of proteins. However, in light of the unique symmetry of the ATPase, it is unlikely that the detailed structure of the proteins is similar and thus it may not be surprising that the immunological relatedness is weak.

The groEL/groES, hsp60 and Rubisco subunit binding protein complexes have recently been shown to serve as molecular chaperonins (Hemmingsen *et al.*, 1988; Goloubinoff *et al.*, 1989a,b; Ostermann *et al.*, 1989). These are proteins which catalyse the correct assembly of oligomeric protein complexes and the unfolding and refolding of aberrantly folded proteins which are generated as a result of physiological stress, such as heat shock (Pelham, 1986; Rothman, 1989). In addition, groEL/groES apparently maintains certain polypeptides destined to be secreted from the cell in an export-competent unfolded or partially folded state until they are able to enter the secretion machinery in the cytoplasmic membrane (Bochkareva *et al.*, 1988; Lecker *et al.*, 1989). This raises the interesting possibility that the ATPase complex might serve a molecular chaperonin function in thermophilic archaebacteria. In organisms which live at such extreme temperatures, one can imagine that a high level of both constitutive and heat shock-inducible (un)foldase activity might be required to maintain cellular proteins in a correctly folded state. This, in addition to structural features of thermophilic enzymes which lend them greater intrinsic stability (Jaenicke and Závodszky, 1990), may help to explain the ability of extremely thermophilic archaebacteria to thrive at high temperature. Thus we postulate that the ATPase complex may represent a novel type of chaperonin related to members of the groEL/hsp60 family but distinguished from them by its unique four-fold or pseudo-eight-fold symmetry, the possession of two distinct subunits, a high basal level of expression (at least 4 times that of groEL) and the ability to function at extremely high temperatures. Experiments to test this hypothesis are underway.

Materials and methods

Bacterial strains

Archaeoglobus fulgidus VC-16 (DSM 4304), *Pyrodictium brockii* S1 (DSM 2708) and *Pyrodictium occultum* PL-19 (DSM 2709) were obtained from our own cultures at the University of Regensburg. *Thermoplasma acidophilum* cells were kindly supplied to us by W.Zillig of the Max-Planck Institute for Biochemistry.

Cell culture

P.occultum was grown in a 300 l fermentor (HTE, Bioengineering, Wald, Switzerland) in thiosulphate-containing 1/2-SME medium supplemented with 0.05% yeast extract (Stetter *et al.*, 1983) at pH 6.0 and 98°C under an H_2/CO_2 (80:20) gas phase at a pressure of 300 kPa and a stirring rate of 70 min^{-1}. When the cell concentration reached 5 × 10^7/ml, the culture was cooled to 4°C by means of a heat exchanger (Fa. Schmidt, Bretten, Germany) and harvested in a Padberg continuous-flow centrifuge. A single fermentation yielded 10–15 g cells (wet wt). The cells were stored at −20°C. *P.brockii* was grown anaerobically as above in the same medium containing sulphur rather than thiosulphate at 105°C in 100 ml serum bottles without stirring, and harvested in the late exponential phase.

A.fulgidus cells were grown under strictly anaerobic conditions in MGG medium (Huber *et al.*, 1982) supplemented with yeast extract (0.5%) and L(+)-lactate (0.1%) at 85°C under an N_2/CO_2 gas phase, and harvested by centrifugation in the exponential growth phase.

Reagents

All reagents were analytical grade and obtained from Sigma or Merck, with the exception of ATP which was purchased from Boehringer Mannheim.

Crude preparations of complex

A dense suspension of freshly grown *P.brockii* cells (400 μl) in 1/2-SME medium lacking sulphur and containing 100 μg/ml DNase was subjected to three cycles of freezing at −20°C and rapid thawing with vortexing in a 35°C water bath. The suspension was diluted 10-fold with CM buffer (10 mM sodium cacodylate pH 5.5, 5 mM $MgCl_2$) containing 50 μg/ml DNase, incubated at RT for 15 min to allow the DNase to work and centrifuged at 39 000 *g* for 15 min at 2°C to sediment cell envelopes and unbroken cells. The pellet was washed twice, resuspended in 2 ml of CM buffer and used immediately to prepare grids for electron microscopy.

A dilute suspension of *A.fulgidus* cells in MGG medium was frozen by plunging into liquid N_2 and allowed to thaw at RT. DNase was added to 10 μg/ml and the suspension incubated at 37°C for 1 h. Envelopes and cells were removed by sedimentation at 15 000 *g* for 10 min and the supernatant used to prepare grids.

Soluble protein fractions of bacterial and yeast cells for ATPase purification, immunoblotting and heat shock experiments were prepared by disrupting the cells with a French press (American Instrument Co., Silver Spring, MD, USA) at a pressure of 630 p.s.i. and retaining the supernatant after removing envelopes and unbroken cells by centrifugation at 39 000 *g* for 40 min at 4°C.

Purification of P.occultum complex

Frozen cells (20 g) were thawed and suspended in 10 mM sodium cacodylate pH 7.0, 5 mM $MgCl_2$. Membrane-free French press lysate was prepared and applied at 1 mg protein per ml bed volume to a DEAE–Sephacel anion exchange column which was equilibrated in TM buffer (10 mM Tris–Cl pH 7.0, 5 mM $MgCl_2$) containing 50 mM KCl at 4°C. The column was developed with a linear gradient of 50–500 mM KCl in TM buffer. Fractions containing the complex were pooled and loaded on a linear density gradient consisting of 10–30% (w/v) sucrose and 5–10% (w/v) glycerol in TM buffer. The gradient was centrifuged in a Beckman SW41Ti rotor (Beckman L5-50 or Centrikon T-2055 ultracentrifuge) at 134 000 *g* and 2°C for 20 h. Complex-containing fractions were pooled and resolved on a linear gradient of 18–37% (w/v) glycerol in TN buffer (50 mM Tris–Cl pH 7.0, 50 mM NaCl), under the same centrifugation conditions as above. A pool of the desired fractions was chromatographed on a Mono-S cation exchange FPLC column (Pharmacia). The column was equilibrated in TN buffer at RT and the sample applied at 1 mg protein per ml bed volume. FPLC was performed at a pressure of 1500 kPa. The complex passed through the column without binding and was collected in the flow-through. Bound proteins were eluted with a linear gradient of 0.05–1.0 M NaCl in 50 mM Tris–Cl pH 7.0. Fractions at each stage were analysed by electron microscopy and SDS–PAGE and assayed for ATPase activity. Prior to each step of the purification procedure, the crude extract or fraction pool was concentrated by ultrafiltration in an Amicon stirred cell with a mol. wt cut-off of 10 000, and dialysed against the next buffer. The purified complex was stable with

respect to ATPase activity for several months when stored in TN buffer containing 30% glycerol at 0°C.

Electrophoresis and immunoblotting

SDS–PAGE was performed according to Laemmli (1970), using gels with a linear gradient of 5–25% acrylamide. Samples were heated at 95°C for 5 min in sample buffer prior to loading on the gel. Densitometry of gel bands was performed by digitizing a photographic negative of the gel and analyzing the resultant image in the SEMPER system (see Image Processing).

Immunoblotting was performed essentially as described by Towbin *et al.* (1979) and Burnette (1981). After transfer of proteins to the nitrocellulose membranes, the membranes were incubated with antiserum raised against the *Pyrodictium* ATPase complex for 2 h at 37°C, followed by alkaline phosphatase-conjugated goat anti-rabbit immunoglobulin G (Sigma). Bound antibody was detected by the addition of 0.17 mg/ml 5-bromo-4-chloro-3-indolyl-phosphate and 0.33 mg/ml nitro-blue tetrazolium in 100 mM Tris–Cl pH 9.5, 100 mM NaCl, 50 mM $MgCl_2$, which produces a purple colour when the phosphate is liberated by hydrolysis.

Protein determination

Protein was determined by the microanalysis procedure of Heil and Zillig (1970).

Preparation of antiserum against the P.occultum complex

Antiserum was raised in a male rabbit by injection of a 1:1 (v/v) emulsion of the purified complex in Freund's complete adjuvant. Six injections of 20 μg protein each were administered subcutaneously in the back at intervals of one week, followed by a single intraperitoneal booster of 60 μg one week later. After another week, 35 ml of blood was taken from the large ear vein. Serum was stored at −20°C. Antibody specificity was determined by Ouchterlony double immunodiffusion in a gel consisting of 1% agarose in phosphate-buffered saline (Williams and Chase, 1971).

ATPase assay

The assay mixture consisted of 22.5 mM Tris–Cl pH 7.5, 0.63 μM ATP, 9 mM $MgCl_2$ and 5 μl of solution containing the enzyme complex, in a total volume of 100 μl. The time and temperature of incubation are given in the figure legends; routine assays were incubated at 90°C or 100°C for 1 min. At temperatures of 100°C or higher, samples were incubated in closed capillaries in a glycerol bath. The reaction was terminated by rapid cooling to 0°C in an ice bath. Residual ATP was determined with a luciferin–luciferase system (ATP Bioluminescence CLS, from Boehringer Mannheim), using a Lumac Biocounter (Abimed, Düsseldorf, Germany) to measure luminescence. For this purpose, 50 μl of luciferase solution (1.7%, w/v) was added to 10 μl of the incubation mixture. Controls containing no enzyme were used to determine the rate of spontaneous hydrolysis of ATP by water, which was subtracted to obtain the enzyme-catalysed rate. One unit of ATPase activity is defined as 1 μmol ATP hydrolysed/min.

Heat shock

To investigate constitutive protein production as a function of growth temperature, cultures were grown from inocula in serum bottles at 90°C and 100°C in hot-air incubators (Heraeus). At the end of exponential phase (30 h at 90°C and 24 h at 100°C) the cultures were cooled in an ice bath and harvested. For growth at 108°C, the culture was incubated in a 50 l fermentor in order to obtain sufficient cell mass since the yield is very low at this temperature. At the end of exponential phase (35 h) the culture was rapidly cooled and harvested.

Heat shock experiments were conducted as follows: A 100 l fermentor culture was grown to exponential phase (21 h) at 102°C. A 2 l sample was harvested. Samples of 1.6 l each were transferred to bottles, gassed with H_2/CO_2 (150 kPa) and further incubated in a hot-air incubator at 102°C for 1 h or 4 h. The remaining fermentor culture was incubated at 108°C. Samples of 2 l each were taken after 1 h, 2 h and 3 h, and the rest of the fermentor culture harvested after 4 h. All samples were rapidly cooled prior to harvest. In both types of experiments, membrane-free French press cell lysates were prepared and subjected to SDS–PAGE, loading an equal quantity of total protein in each well.

Electron microscopy

A droplet of sample (cell envelope suspension, crude cytoplasmic extract or purification fraction) was applied to a glow-discharged carbon-coated copper grid. In the case of fractions from the purification protocol, a small aliquot of the sample was first dialysed against buffer. After allowing the envelopes and/or protein to adsorb for 1–2 min, the grid was rinsed on droplets of deionized water and stained with 2% uranyl acetate (pH 4) or 2% ammonium molybdate. Electron microscopy was performed with a Philips EM420 at an operating voltage of 80 kV and nominal magnification of 36 000× or 49 000×.

Image processing

Images were digitized as arrays of 1024 × 1024 pixels with a flat bed densitometer at a pixel size of 20 μm, corresponding to 0.42 nm or 0.57 nm at the specimen level. Alternatively, an Eikonix model 1412 camera system (Eikonix Corporation, Bedford, MA, USA) was used at a pixel size of 15 μm, equivalent to 0.42 nm at the specimen level. Image processing was performed using the EM (Hegerl and Altbauer, 1982) and SEMPER systems (Saxton *et al.*, 1979). Images of individual particles were selected interactively using Metheus Omega 445 or 3610 graphics-raster display systems (Metheus Corporation, Hillsboro, OR, USA). The images were aligned with respect to translation and orientation using cross-correlation methods and averaged. An arbitrarily chosen reference was used for the first cycle of alignment and averaging, and the resulting average used as a reference in a second refinement cycle. Further refinement passes were made if they resulted in an increase in resolution and in the values of the cross-correlation coefficients. Circular or rectangular soft-edged masks were applied to the particle images to minimize the effect of spurious background features on the alignment.

Rotational correlation plots for individual particle images were obtained in the SEMPER system using a program written by Roland Dürr (Max-Planck Institute for Biochemistry).

Acknowledgements

We wish to thank Günter Pfeifer, Susanne Volker and Ute Santarius for excellent technical assistance in the electron microscopy and image processing, Peter Hummel for his invaluable help in the biochemical studies, and Frank Pitzer for helpful discussions. B.M.P. was the recipient of a Medical Research Council of Canada postdoctoral fellowship.

References

Arrigo,A.-P., Simon,M., Darlix,J.-L. and Spahr,P.-F. (1987) *J. Mol. Evol.*, **25**, 141–150.

Baumeister,W., Dahlmann,B., Hegerl,R., Kopp,F., Kuehn,L. and Pfeifer,G. (1988) *FEBS Lett.*, **241**, 239–245.

Bochkareva,E.S., Lissin,N.M. and Girshovich,A.S. (1988) *Nature*, **336**, 254–257.

Burnette,W.N. (1981) *Anal. Biochem.*, **112**, 195–203.

Costantino,H.R., Brown,S.H. and Kelly,R.M. (1990) *J. Bacteriol.*, **172**, 3654–3660.

Dahlmann,B., Kopp,F., Kuehn,L., Niedel,B., Pfeifer,G., Hegerl,R. and Baumeister,W. (1989) *FEBS Lett.*, **251**, 125–131.

Darland,G., Brock,T.D., Samsonoff,W. and Conti,S.F. (1970) *Science*, **170**, 1416–1418.

Eggen,R., Geerling,A., Watts,J. and de Vos,W.M. (1990) *FEMS Microbiol. Lett.*, **71**, 17–20.

Feldman,S.R., Gonias,S.L. and Pizzo,S.V. (1985) *Proc. Natl. Acad. Sci. USA*, **82**, 5700–5704.

Goloubinoff,P., Christeller,J.T., Gatenby,A.A. and Lorimer,G.H. (1989a) *Nature*, **342**, 884–889.

Goloubinoff,P., Gatenby,A.A. and Lorimer,G.H. (1989b) *Nature*, **337**, 44–47.

Hegerl,R. and Altbauer,A. (1982) *Ultramicroscopy*, **9**, 109–116.

Heil,A. and Zillig,W. (1970) *FEBS Lett.*, **11**, 165–168.

Hemmingsen,S.M., Woolford,C., van der Vies,S.M., Tilly,K., Dennis,D.T., Georgopoulos,C.P., Hendrix,R.W. and Ellis,R.J. (1988) *Nature*, **383**, 330–334.

Hendrix,R.W. (1979) *J. Mol. Biol.*, **129**, 375–392.

Herendeen,S.L., VanBogelen,R.A. and Neidhardt,F.C. (1979) *J. Bacteriol.*, **139**, 185–194.

Hohn,T., Hohn,B., Engel,A., Wurtz,M. and Smith,P.R. (1979) *J. Mol. Biol.*, **129**, 359–373.

Huber,H., Thomm,M., König,H., Thies,G. and Stetter,K.O. (1982) *Arch. Microbiol.*, **123**, 47–50.

Huber,R., Kurr,M., Jannasch,H.W. and Stetter,K.O. (1989) *Nature*, **342**, 833–834.

Hutchinson,E.G., Tichelaar,W., Hofhaus,G., Weiss,H. and Leonard,K.R. (1989) *EMBO J.*, **8**, 1485–1490.

Jaenicke,R. and Závodszky,P. (1990) *FEBS Lett.*, **268**, 344–349.

Jerez,C.A. (1988) *FEMS Microbiol. Lett.*, **56**, 289–294.
Klenk,H.-P., Haas,B., Schwass,V. and Zillig,W. (1986) *J. Mol. Evol.*, **24**, 167–173.
Kopp,F., Steiner,R., Dahlmann,B., Kuehn,L. and Reinauer,H. (1986) *Biochim. Biophys. Acta*, **872**, 253–260.
Laemmli,U.K. (1970) *Nature*, **227**, 680–685.
Lecker,S., Lill,R., Ziegelhoffer,T., Georgopoulos,C., Bassford,P.J.,Jr., Kumamoto,C.A. and Wickner,W. (1989) *EMBO J.*, **8**, 2703–2709.
Lemaux,P.G., Herendeen,S.L., Bloch,P.L. and Neidhardt,F.C. (1978) *Cell*, **13**, 427–434.
Lilley,K.S., Davison,M.D. and Rivett,A.J. (1990) *FEBS Lett.*, **262**, 327–329.
Lindquist,S. (1986) *Annu. Rev. Biochem.*, **55**, 1151–1191.
Martel,R., Cloney,L.P., Pelcher,L.E. and Hemmingsen,S.M. (1990) *Gene*, **94**, 181–187.
McMullin,T.W. and Hallberg,R.L. (1987) *Mol. Cell. Biol.*, **7**, 4414–4423.
McMullin,T.W. and Hallberg,R.L. (1988) *Mol. Cell. Biol.*, **8**, 371–380.
Musgrove,J.E., Johnson,R.A. and Ellis,R.J. (1987) *Eur. J. Biochem.*, **163**, 529–534.
Neidhardt,F.C. and VanBogelen,R.A. (1987) In Neidhardt,F.C., Ingraham,J.L., Low,K.B., Magasanik,B., Schaechter,M. and Umbarger,H.E. (eds), *Escherichia coli and Salmonella typhimurium: Cellular and Molecular Biology*. American Society for Microbiology, Washington, Vol. 1, pp. 1334–1345.
Neidhardt,F.C., Phillips,T.A., VanBogelen,R.A., Smith,M.W., Georgalis,Y. and Subramanian,A.R. (1981) *J. Bacteriol.*, **145**, 513–520.
Ostermann,J., Horwich,A.L., Neupert,W. and Hartl,F.-U. (1989) *Nature*, **341**, 125–130.
Pelham,H.R.B. (1986) *Cell*, **46**, 959–961.
Pihl,T.D., Schicho,R.N., Kelly,R.M. and Maier,R.J. (1989) *Proc. Natl. Acad. Sci. USA*, **86**, 138–141.
Pragishvilli,D., Zillig,W., Gierl,A., Biesert,L. and Holz,I. (1982) *Eur. J. Biochem.*, **122**, 471–477.
Pushkin,A.V., Tsuprun,V.L., Solovjeva,N.A., Shubin,V.V., Evstigneeva,Z.G. and Kretovich,W.L. (1982) *Biochim. Biophys. Acta*, **704**, 379–384.
Reading,D.S., Hallberg,R.L. and Myers,A.M. (1989) *Nature*, **337**, 655–659.
Roberts,D.V. (1977) *Enzyme Kinetics*. Cambridge University Press, Cambridge.
Rothman,J.E. (1989) *Cell*, **59**, 591–601.
Saxton,W.O., Pitt,T.J. and Horner,M. (1979) *Ultramicroscopy*, **4**, 343–354.
Siegel,V. and Walter,P. (1988) *Trends Biochem. Sci.*, **13**, 314–316.
Stetter,K.O. (1982) *Nature*, **300**, 258–260.
Stetter,K.O. (1988) *System. Appl. Microbiol.*, **10**, 172–173.
Stetter,K.O., Thomm,M., Winter,J., Wildgruber,G., Huber,H., Zillig,W., Janécovic,D., König,H., Palm,P. and Wunderl,S. (1981) *Zbl. Bakt. Hyg., I. Abt. Orig. C*, **2**, 166–178.
Stetter,K.O., König,H. and Stackebrandt,E. (1983) *System. Appl. Microbiol.*, **4**, 535–551.
Stetter,K.O., Lauerer,G., Thomm,M. and Neuner,A. (1987) *Science*, **236**, 822–824.
Towbin,H., Staehelin,T. and Gordon,J. (1979) *Proc. Natl. Acad. Sci. USA*, **76**, 4350–4354.
Trent,J.D., Osipiuk,J. and Pinkau,T. (1990) *J. Bacteriol.*, **172**, 1478–1484.
Viitanen,P.V., Lubben,T.H., Reed,J., Goloubinoff,P., O'Keefe,D.P. and Lorimer,G.H. (1990) *Biochemistry*, **29**, 5665–5671.
Williams,C.A. and Chase,M.W. (1971) *Methods Immunol. Immunochem.*, **3**, 146–160.
Woese,C.R., Kandler,O. and Wheeler,M.L. (1990) *Proc. Natl. Acad. Sci. USA*, **87**, 4576–4579.
Zillig,W., Holz,I., Janekovic,D., Klenk,H.-P., Imsel,E., Trent,J., Wunderl,S., Hugo Forjaz,V., Coutinho,R. and Ferreira,T. (1990) *J. Bacteriol.*, **172**, 3959–3965.

Received on February 18, 1991; revised on March 25, 1991